

<sup>1</sup> Wageningen University, Meteorology and Air Quality Group, Wageningen, The Netherlands

<sup>2</sup> University of Idaho at Kimberly Research and Extension Center, Kimberly, Idaho, USA

## Regional Advection Perturbations in an Irrigated Desert (RAPID) experiment

H. A. R. De Bruin<sup>1</sup>, O. K. Hartogensis<sup>1</sup>, R. G. Allen<sup>2</sup>, and J. W. J. L. Kramer<sup>1</sup>

With 12 Figures

Received October 17, 2003; accepted July 10, 2004

Published online November 17, 2004 © Springer-Verlag 2004

### Summary

The RAPID field experiment took place in August–September 1999 at a site 25 km south of Twin Falls, Idaho, USA. The experiment concerned micrometeorological observations over extensive, well-irrigated fields covered with the fast-growing crop alfalfa. During daytime, on a number of days the sensible heat flux was negative and the latent heat flux exceeded net radiation. The energy required for the latent heat flux to be larger than net radiation has to be advected from elsewhere. As the fields were large, we refer to this process as “*regional advection*”. “*Local advection*”, on the other hand, refers to advection effects, where the wet to dry transition is on a field scale. Evidence is presented that the RAPID data are subject to regional advection conditions.

A simple model, based on Penman-Monteith, is derived that describes the regional-advection case rather well. The influence of wind speed under those conditions is illustrated using data and the model. The correlation coefficients between temperature and horizontal wind component appear to be good indicators for advection.

### 1. Introduction

Evapotranspiration,  $ET$ , or expressed in energy units,  $\lambda ET$ , where  $\lambda$  is the latent heat of vaporization, is generally some fraction of net radiation,  $R_n$ , for climates that have sufficient rainfall to support  $ET$ . In areas where the air mass is strongly modified by dry, desert conditions, however, the

ratio of  $\lambda ET$  to  $R_n$  can exceed 2. Figure 1 illustrates this for Kimberly, Idaho, where lysimeter measurements of 24-hour  $\lambda ET$  of full cover alfalfa divided by the corresponding  $R_n$  are presented. The measured  $\lambda ET$  exceeds the available energy (that is close to  $R_n$  for daily values, because the daily soil heat flux density,  $G$ , is usually small) by 50% for most of August and September. During this period, dry air is advected from the large desert areas upwind of Kimberly.

Considering the surface energy balance,

$$R_n - G = \lambda ET + H \quad (1)$$

one can see that under the conditions mentioned above, i.e.  $\lambda ET > R_n$  and  $G$  is negligible, the sensible heat flux density,  $H$ , must be negative. The required additional energy, needed to maintain the high evaporation rate, must be supplied by extracting sensible heat from the lower atmosphere.

If we consider large horizontally homogeneous fields where the atmospheric flow is in equilibrium with the underlying surface, the air temperature and humidity in the atmospheric surface layer are well adapted to the irrigated field and no longer have the properties of the dry upwind terrain. Crucial for our considerations is that a negative  $H$  implies that the atmosphere just above the surface is stably stratified and the

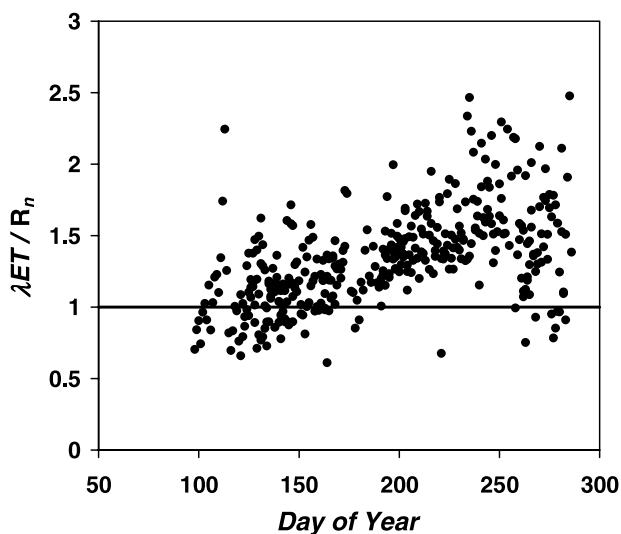


**Fig. 1.** Daily fraction of evapotranspiration,  $\lambda ET$ , to net radiation,  $R_n$ , versus Day of Year. Daily  $\lambda ET$  is based on lysimeter data, taken at Kimberly, Idaho between 1969 and 1971

negative buoyancy effects suppress turbulent motions. The turbulence needed for vertical transfer of water vapour, therefore, can only be generated in a mechanical way. This means that  $\lambda ET$  can exceed  $R_n$  only if there is enough wind to offset the damping effects of stability. Under calm conditions it is to be expected that daily  $\lambda ET$  cannot exceed  $R_n$ .

For small fields with finite size, on the other hand, things become more complicated. We define a small field as a field where under certain conditions the wind fetch is too small to adapt the advected, dry air mass to the irrigated surface. In that case, at any distance from the edge separating the irrigated field and the dry upwind desert, the influence of the upwind dry terrain will increase with increasing wind speed. For that reason  $\lambda ET$  is expected to increase with increasing wind speed due to the fact that dry desert air is forced to flow over the wet irrigated surface.

From this common sense reasoning, we deduce that  $\lambda ET$  of irrigated fields in dry deserts is enhanced by wind in two ways:

1. For large fields, i.e. large in the sense that the flow has adapted to the irrigated surface, wind enhances the mechanically generated turbulence needed to maintain vertical transfer under stable conditions. This is denoted as regional advection;
2. For small fields, i.e. small in the sense that the flow has not been fully adapted to the irri-

gated field, wind forces dry, 'non-adapted' desert air over the irrigated field, which enhances evaporation. This case is often called local advection.

Considering vertical exchange of eddies or air parcels under conditions that  $H < 0$  and  $\lambda ET > 0$ , it is expected that upward moving eddies contain relatively cool and wet air, whereas downward moving parcels will be warm and dry. Consequently, the correlation coefficient of turbulent temperature and humidity measurements,  $R_{Tq}$ , is expected to be negative. Conversely, under 'normal' conditions, i.e. both  $H$  and  $\lambda ET$  are  $> 0$ ,  $R_{Tq}$  is expected to be positive. So,  $R_{Tq}$  seems an appropriate indicator for advection conditions. Also correlation coefficients between horizontal wind speed and temperature and humidity might be good indicators.

In the past a lot of work has been done on the behaviour of turbulent flow just after a sudden dry-to-wet step-change at the surface, i.e. local advection. In that case, the flow is not in equilibrium with the underlying surface and, e.g. Monin-Obukhov similarity theory breaks down (see for instance Kroon and DeBruin, 1995; Bink, 1995 and more recent studies by e.g. McNaughton and Laubach, 2000).

It is the purpose of the RAPID field experiment to gather micrometeorological data over a large irrigated field surrounded by very dry terrain. In this paper we will present some first results of the effect of wind speed on  $\lambda ET$  under advection conditions. In addition, we will discuss the relation between some statistical quantities, such as  $R_{Tq}$ , and advection.

## 2. Experimental

The RAPID experiment was carried out between 25 August and 19 September 1999 in an agricultural area of  $70 \times 25$  km, located in Idaho, USA, 20 km south-east of Twin Falls. Staff members of the University of Idaho, Wageningen University, Campbell Scientific, Inc., Utah State University and USDA-ARS, Kimberly, Idaho, participated in RAPID. Four eddy-correlation systems were deployed, all consisting of CSAT3 sonic anemometer and a KH20 Krypton hygrometer, both from Campbell Scientific Inc., Logan, USA. Measurements were recorded by a Campbell

Scientific CR23X datalogger. Raw data were stored on a laptop and processed afterwards. In addition, two Bowen ratio systems and sensors to measure the components of the net radiation (CM14 pyranometer and CG2 pyrgeometer of Kipp and Zonen, Delft, the Netherlands), surface temperature (Everest 4000 infra-red thermometers, Tucson, USA) and soil heat flux (REBS HFT3 soil heat flux plates) were installed. During RAPID also a net radiometer manufactured by Swissteco has been operated. We adopted the results of a study in the Netherlands (Kohsiek, personal communication) that revealed that the 4-component Kipp and Zonen system provides the ‘correct’ net radiation values. Moreover, this has been confirmed by a detailed study by Kramer (2000), who compared data for all available RAPID radiation data. We estimate that the errors made in net radiation are less than 5%. Missing Kipp and Zonen data were replaced with observations made with the Swissteco radiometer accounting for the systematic difference of 8% found for this sensor compared with the Kipp and Zonen system. Kramer (2000) also analysed all available data concerning soil temperature and soil heat flux and determined the ‘best’ soil heat flux accounting for e.g. the heat storage in the layer between the surface and the soil heat flux plates. In this paper we will use mainly data of the eddy-correlation system operated at 3 m by Wageningen University. The micrometeorological equipment was installed between two centre-pivot irrigated alfalfa fields of approximately 1 mile by 1 mile. Towards the west, the dominant wind direction, beyond the field adjacent to the equipment, two more irrigated fields, of respectively alfalfa and wheat were grown. We can thus assume that the experimental area is large in terms of the definitions given in Section 1. The alfalfa crop height varied for the field west of our equipment between 10 cm at the start of the experiment to about 35 cm at the end, and between 15 and 35 cm at the east field. For more details on the RAPID experiment, see Kramer (2000).

The eddy-correlation data were processed to get 30 minute averaged fluxes using the latest version of the EC-pack software package, developed by the Wageningen University. The source code and documentation of the software can be found at [www.met.wau.nl](http://www.met.wau.nl).

The eddy-correlation data at 3 m appear not to fulfil energy balance closure, i.e.  $R_n - G > \lambda ET + H$ . We corrected for this effect by multiplying both the measured  $H$  and  $\lambda ET$  with a constant factor of 1.5. In this way our data artificially close the energy balance. We realize that our approach is very arbitrarily and that other correction procedures can be applied also. Recently, the significance of the energy balance closure problem has been recognized internationally. It is outside the scope of this study to deal with this issue here. We confine ourselves to refer to a recent review paper by Culf et al. (2004).

### 3. Model

The aim of this paper is to illustrate the effect of wind speed on  $\lambda ET$  under advection conditions. For small fields there is still no simple theoretical approach, and will not be discussed here in detail. For large fields we will derive a simple model based on the Penman-Monteith method. We start with the governing equations on which Penman-Monteith is based. Besides Eq. (1) these are:

$$R_n = (1 - \alpha)K^\downarrow + \varepsilon_s(L^\downarrow - \sigma T_s^4) \quad (2)$$

$$H = \rho c_p \frac{T_s - T}{r_a} \quad (3)$$

$$\lambda ET = \frac{\rho c_p e_s(T_s) - e}{\gamma r_a + r_s} \quad (4)$$

where  $\alpha$  is the albedo,  $K^\downarrow$  and  $L^\downarrow$  the incoming short- and long-wave radiation,  $\sigma$  the Stefan-Boltzmann constant,  $\varepsilon_s$  emissivity of the surface,  $T_s$  the surface temperature,  $\rho$  and  $c_p$  the density and specific heat at constant pressure of air,  $T$  and  $e$  the temperature and water vapour pressure of the air at standard level,  $\gamma$  the so-called psychrometer constant and  $r_a$  and  $r_s$  the aerodynamic and surface resistance. It is important to note that we account for stability effects on  $r_a$  by using an iterative calculation scheme based on the Monin-Obukhov similarity theory (MOST), including the buoyancy effect of water vapour. In this procedure the roughness length for momentum and heat,  $z_{0m}$  and  $z_{0h}$  play a role. We used the standard MOST functions of Businger-Dyer for unstable and those of Beljaars and Holtslag for stable cases (see Dyer, 1974; Beljaars and Holtslag, 1991 and Holtslag and DeBruin, 1988). The set of Eqs. (1) to (4) is solved for

$H$ ,  $\lambda ET$  and  $T_s$  at given  $K^\downarrow$  and  $L^\downarrow$ ,  $G$ ,  $T$ ,  $e$ ,  $\alpha$ ,  $\varepsilon_s$ ,  $r_s$ ,  $z_{0m}$  and  $z_{0h}$  using a numerical iterative scheme. For this purpose we used the standard MOST expressions for  $r_a$  that, in its turn, is dependent on the friction velocity, the Obukhov-length, the observation height and the roughness parameters  $z_{0m}$  and  $z_{0h}$  (see e.g. Stewart et al., 1994). Note that through Eq. (2) we account also for the influence of surface temperature on net radiation. We used the measured soil heat flux density.

We will apply this simple model for some selected ‘advection’ days during RAPID using the measured  $K^\downarrow$  and  $L^\downarrow$ ,  $G$ ,  $T$ ,  $e$  and wind speed, in order to see whether the model is able to describe the advection conditions properly. Next we will apply the model as a prognostic tool to

investigate the effects of wind speed on  $\lambda ET$ . We repeat that the model applies to large fields only.

## 4. Results

### 4.1 Energy balance

In Fig. 2 the various components of the energy balance and the wind speed at 3 m are depicted for a day with low wind speed. Note that  $H$  and  $\lambda ET$  have been corrected according to the procedure described in Section 2. It is seen that  $H$  is positive and  $\lambda ET < R_n$ .

In Fig. 3 the same quantities are plotted but now for two successive days with daytime wind speed at 3 m greater than  $3 \text{ m s}^{-1}$ .  $H$  is negative both during day- and night-time and  $\lambda ET$  is

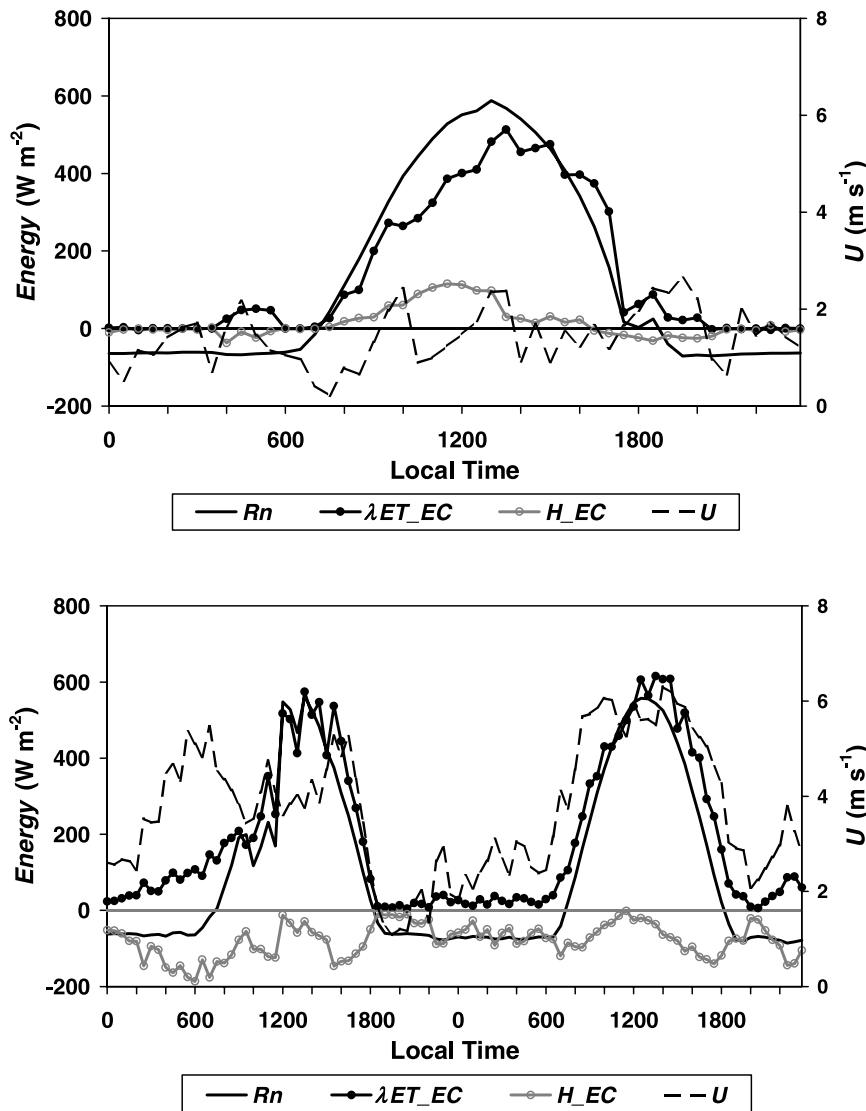


**Fig. 2.** Diurnal cycle of net radiation,  $R_n$ , sensible heat flux,  $H$  and evapotranspiration,  $\lambda ET$  on a calm day (DOY 247) during RAPID. The eddy-correlation determined  $H$  and  $\lambda ET$  are corrected for energy balance closure as described in Section 2

**Fig. 3.** As Fig. 2, for two consecutive days with high wind speed (DOY 253 and 254)

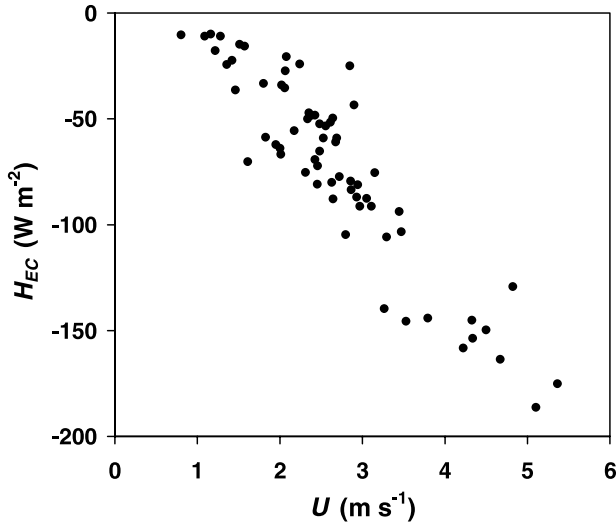


**Fig. 4.** Night-time (between 19:00 and 7:00) measured sensible heat flux at 3 m,  $H$ , against wind speed,  $u$ , for DOY 252 19:00 to 255 7:00. The eddy-correlation determined  $H$ , has been corrected for energy balance closure as described in Section 2

greater  $R_n$ , and at night greater than 0. Under night-time conditions  $H$  and  $G$  are the only available energy sources to feed  $\lambda ET$  as  $R_n$  is negative. This means that  $H$  must be negative, i.e. directed towards the surface, and, consequently, the stratification is stable.  $H$  is then expected to be related directly to wind speed, as wind is the only turbulence generator. In Fig. 4 this feature is illustrated by plotting for the same data set the night-time values of  $H$  against  $u$ . It is seen that  $H$  is related almost linearly to  $u$ .

In Fig. 5 the modelled and measured  $H$  and  $\lambda ET$  are compared for the same period depicted

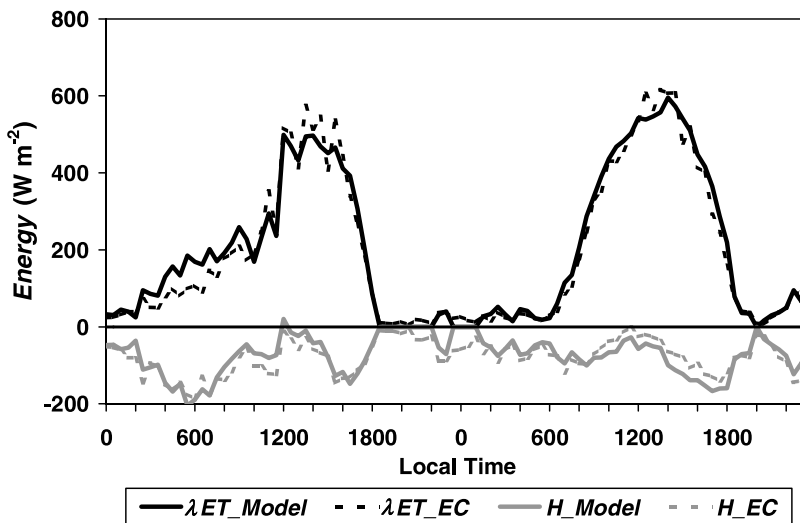


**Fig. 5.** Modelled and measured sensible heat flux,  $H$  and evapotranspiration,  $\lambda ET$ , versus Day of Year (DOY) for DOY 253 and 254. The eddy-correlation determined  $H$  and  $\lambda ET$ , have been corrected for energy balance closure as described in Section 2

in Fig. 3. We ‘tuned’ the model, i.e. we have chosen by trial-and-error,  $r_s$ ,  $z_{0m}$  and  $z_{0h}$ , in such a way that the model agrees best with the measurements. We found  $r_s = 20 \text{ s m}^{-1}$  for  $R_n - G > 0$  (daytime) and  $r_s = 120 \text{ s m}^{-1}$  otherwise (night-time),  $z_{0m} = 0.005 \text{ m}$  and  $z_{0h} = z_{0m}/10$  and used  $\varepsilon_s = 0.98$ . These values correspond fairly well with those found for alfalfa by Walter et al. (2002).

In Figs. 6 and 7 we compared the modelled and measured values of  $H$  and  $\lambda ET$  respectively. The calculated and observed surface temperatures are compared in Fig. 8. Although with some scatter, especially for  $H$ , the overall picture is that the tuned model describes the selected high-wind situation well. This is supported by Fig. 9, where the modelled  $H$  is plotted against  $u$  for the night-time conditions similarly to Fig. 4 for measured  $H$ . It is seen that the results compare well with the observations depicted in Fig. 3.

#### 4.2 Some statistical quantities

We analysed also the correlation coefficients between temperature,  $T$ , and specific humidity,  $q$ , as well as the correlation coefficients between the horizontal wind vector,  $u$ , and  $T$  and  $q$ . In Fig. 10, the correlation coefficients  $R_{Tq}$ ,  $R_{uT}$  and  $R_{uq}$  are plotted for the same days as Figs. 3 and 5. It is seen that  $R_{Tq}$  is negative and approaches at times  $-1$ ,  $R_{uT}$  averages about  $+0.6$  and  $R_{uq}$  about  $-0.6$ . Note that this figure refers to an advection case, so  $H$  is negative, i.e.  $R_{wT} < 0$  and  $\lambda ET$  is positive, i.e.  $R_{wq} > 0$ .

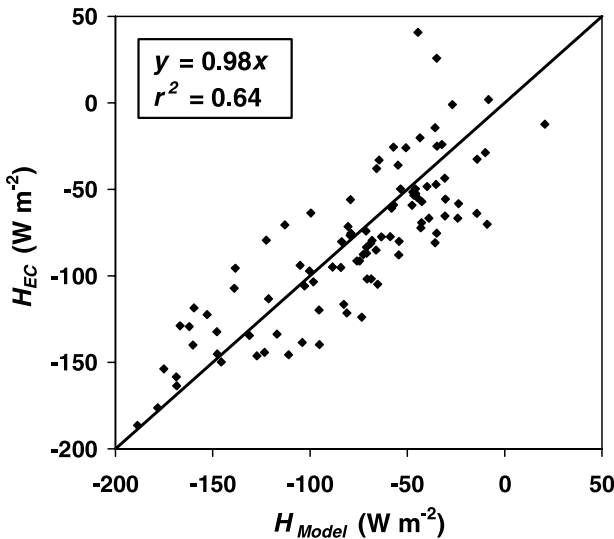


Fig. 6. Modelled versus measured sensible heat flux,  $H$  for DOY 252 19:00 to 255 7:00. The eddy-correlation determined  $H$ , has been corrected for energy balance closure as described in Section 2

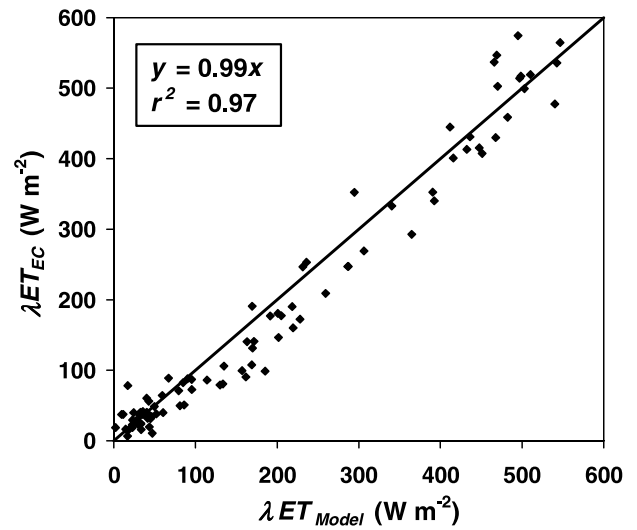


Fig. 7. As Fig. 6, for evapotranspiration,  $\lambda ET$  instead of  $H$

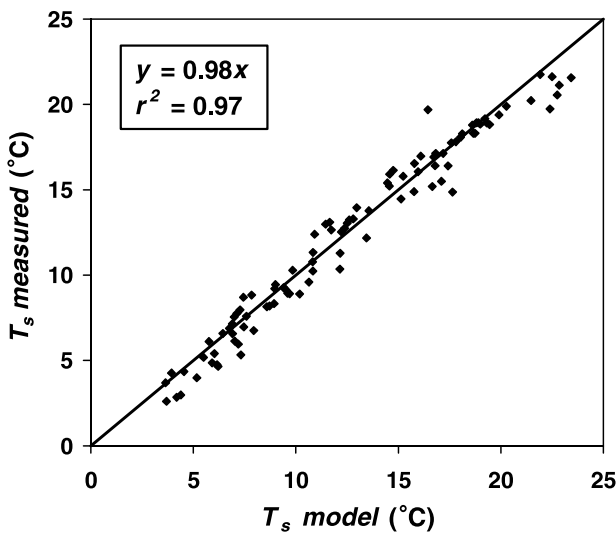


Fig. 8. Modelled versus measured surface temperature for DOY 252 19:00 to 255 7:00

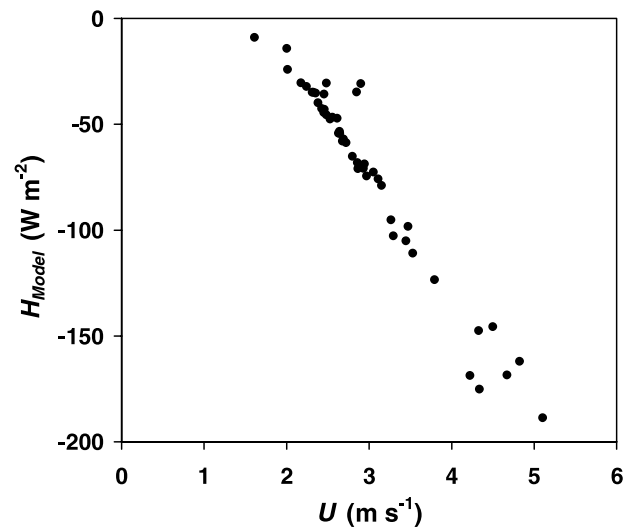


Fig. 9. As Fig. 4, for modelled instead of measured sensible heat flux,  $H$

In Fig. 11  $R_{Tq}$  is plotted against  $R_{uT}$  for the whole experiment with horizontal wind speed at 3 m greater than  $4 \text{ m s}^{-1}$ . It is seen that under these high wind speed conditions  $R_{Tq}$  and  $R_{uT}$  are strongly correlated.

It should be noted that our findings that  $R_{uq}$  and  $R_{uT}$  are connected through  $R_{uw}$  and  $R_{Tq}$  is of course not new. The point we want to make here is that apparently  $R_{uT}$  is an ‘advection’ indicator that might be measurable operationally as discussed in the next section.

## 5. Discussion

We recall that we corrected the measured eddy-correlation fluxes, both  $H$  and  $\lambda ET$ , with a factor 1.5 (see Section 2). As we consider cases where  $H < 0$ , this correction gives a higher  $\lambda ET$  than if we had assumed the measured  $H$  to be correct and  $\lambda ET$  determined as a residual of the energy balance, i.e.  $\lambda ET = R_n - G - H$ .

This study is devoted to regional advection, i.e. we selected an extensive irrigated agricultural fields surrounded by a desert. It was found that

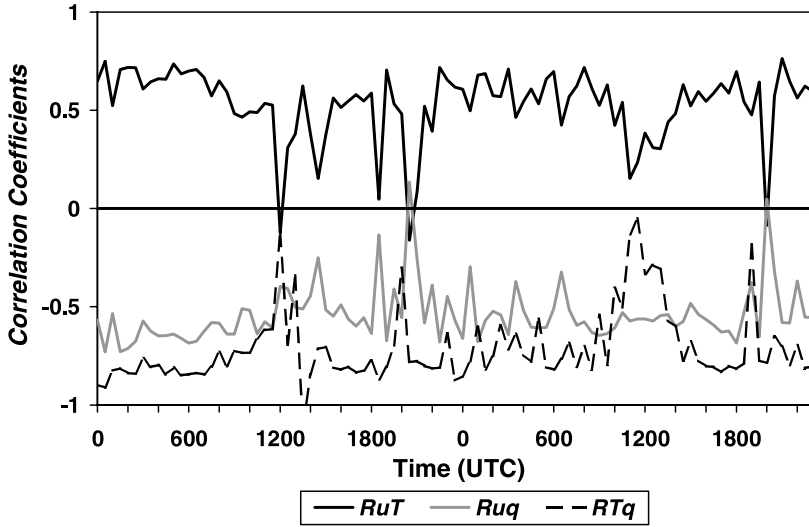


**Fig. 10.** Correlation coefficients between temperature and humidity,  $R_{Tq}$ , wind speed and temperature,  $R_{uT}$  and wind speed and humidity,  $R_{uq}$  for days with high wind speed (DOY 253 and 254)

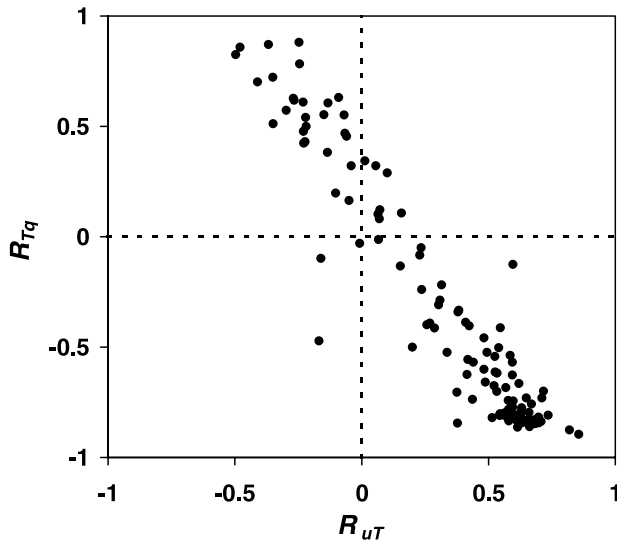


**Fig. 11.** Correlation coefficients between temperature and humidity,  $R_{Tq}$ , wind speed and temperature,  $R_{uT}$  for all RAPID data with wind speed at 3 m larger than  $4 \text{ m s}^{-1}$

actual  $\lambda ET$  can exceed the available energy significantly under these conditions provided that there is sufficient wind. The reason is that  $\lambda ET > R_n$  is possible only if the sensible heat is negative, and, consequently, the air close to the ground is stably stratified. Under those conditions buoyancy suppresses turbulent motions and wind is the only mechanism that can generate the turbulence required for the transport of heat and moisture.

This picture is confirmed by our data of the RAPID experiment. It is found that during night-time, turbulence is absent indeed when wind speed is less than a ‘critical’ value of about

$2 \text{ m s}^{-1}$  (see Figs. 2 and 3). This value will depend on various environmental conditions, for which we will derive an expression. A measure for the ‘critical wind speed’ can be inferred from the bulk-Richardson number,  $R_{ib} \equiv \frac{g}{T_r} z \frac{\Delta T}{u^2}$ , where  $\Delta T = T_s - T$ ,  $g$  the acceleration of gravity,  $T_r$  the absolute temperature of the air layer between the surface and  $z$  and  $u$  the wind speed at  $z$ . Turbulence will vanish if  $R_{ib}$  exceeds its critical value  $R_{ibc}$ . Here we adopt  $R_{ibc} = 0.25$ . Considering the hypothetical case where conditions are just turbulent, then, if  $u$  decreases to its critical value  $u_c$ , turbulence will vanish, and  $H$  and  $\lambda ET$  will be zero (see e.g. Holtslag and DeBruin, 1988). For night-time conditions, the energy budget equation reads  $\varepsilon_s(L^\downarrow - \sigma T_{sc}^4) - G = 0$ , in which  $T_{sc}$  is the ‘critical’ surface temperature. This quantity can be determined from the measured incoming long-wave radiation and soil heat flux adopting a value for  $\varepsilon_s$  (here 0.98). In this way we obtain an expression for the night-time ‘critical’ wind speed,  $u_c$  given by

$$u_c = \sqrt{\frac{g}{T_r} z \frac{T - T_{sc}}{R_{ibc}}}, \quad (5)$$

with  $R_{ibc} = 0.25$ .

For the limited data set we analysed we found  $u_c$  between  $1.5$  and  $3 \text{ m s}^{-1}$ , which corresponds well with our observations (see Fig. 4). Note that in this simple approach the surface roughness does not play a role. Equation 5 can be used to determine  $u_c$  for night-time conditions independent of the surface type. It should be stressed that at low wind speed the stable flow can become intermittent, and

the derived model breaks down. It is outside the scope of this study to dwell on this complicated issue. For recent developments see e.g. Van de Wiel et al. (2001) or Hartogensis et al. (2002).

Our measurements show that during night-time  $\lambda ET$  can reach values up to  $150 \text{ W m}^{-2}$  when wind speed at 3 m is about  $6 \text{ m s}^{-1}$ . This means that if such high wind speed conditions persist for, say, 10 hours,  $\lambda ET$  can be as large as 2 mm per night. This refers to a case in which the surface resistance is very small (we fitted our model to the data with  $r_s = 120 \text{ s m}^{-1}$  for night-time).  $\lambda ET$  of 2 mm per night then refers most likely to direct evaporation of irrigation water, so to periods just after irrigation. Substantial night-time  $\lambda ET$  rates have been observed also with the precision lysimeter at Kimberly (Jim Wright, personnel communication).

During daytime solar heating tends to make the conditions less stable and  $H$  never drops significantly below 0 when the sun is high, i.e. at midday. Moreover, during daytime the wind is not the only turbulence generator and the effect of wind speed on  $\lambda ET$  is less apparent. During overcast conditions the wind effect is expected to be important during daytime also.

The simple model we used reproduces the wind dependence shown in Figs. 4 and 5 as well as the features related to  $R_{ib}$  (not shown) with parameters such as  $z_{0m}$ ,  $z_{0h}$ ,  $\varepsilon_s$  and, above all,  $r_s$  tuned to the measurements. By tuning, we determined that for the advection period  $r_s = 20 \text{ s m}^{-1}$  for  $R_n - G > 0$  (daytime) and  $r_s = 120 \text{ s m}^{-1}$  otherwise (night-time). In literature a minimum value for  $r_s$  of about  $30 \text{ s m}^{-1}$  is given for transpiration of most crops during daytime and a higher value for night-time (see e.g. Walter et al., 2002; Allen et al., 1996).

Our data set does not allow distinguishing between evaporation of liquid irrigation water and transpiration since the eddy-correlation method gives only the total  $\lambda ET$ . It might be possible that a part of the measured  $\lambda ET$  was due to direct evaporation of irrigation water. The centre pivot irrigation system was operating nearly continuously in the field upwind of our measuring systems. In any case, direct evaporation of irrigation water is loss of water resources for agriculture and may not correspond to increase in biomass. Our results might suggest that this loss can be significant at high wind speed. Consequently, it might be wise to recommend that farm-

ers do not irrigate if high wind speed is expected by local weather services, unless it is necessary to sustain soil water above critical values of course.

Since the tuned model gives results that compare well with the observed (corrected) data, and appears to represent a maximum limit of  $\lambda ET$  under wet conditions with advection it might be an alternative to the 'standard' FAO-method based the FAO Irrigation and Drainage Paper No. 56 (Allen et al., 1998) for this type of usage. An important difference is that hourly meteorological data are required, because the diurnal variation of wind speed and stability appear to play important roles.

We showed that the correlation coefficient between (fast) fluctuations of temperature and specific humidity,  $R_{Tq}$ , is a good indicator for advection conditions. Under these conditions,  $H$  is negative and  $\lambda ET$  positive and  $R_{Tq}$  approaches  $-1$ . Note that under 'normal', non-advection conditions during daytime when both  $H$  and  $\lambda ET$  are positive  $R_{Tq}$  appears to be close to one, if the conditions are not too dry (for a detailed discussion see DeBruin et al., 1999). This study revealed that also another statistical quantity might serve as an advection-indicator, namely the correlation coefficient between the horizontal wind speed and temperature,  $R_{uT}$ . At a wind speed greater than  $4 \text{ m s}^{-1}$ ,  $R_{Tq}$  appears to be highly related to  $R_{uT}$  (see Fig. 10). This quantity can be determined with a 2D sonic anemometer, which measures the horizontal wind vector and the so-called sonic-temperature and is a suitable alternative for the standard cup anemometer with wind vane currently used at standard weather stations.

Our results might be the basis for a simple method to determine actual  $\lambda ET$  under night-time advection conditions. First, with the 2D sonic  $R_{uT}$  is determined and next  $R_{Tq}$ . Next, advection situations can be selected for which, in the next step,  $H$  can be estimated using the tuned model. Finally,  $\lambda ET$  can be evaluated as residual from the energy balance equation, using measured  $R_n$  and  $G$ .

So far, we did not discuss the effect of wind in cases of local advection, i.e. when the irrigated fields are too small for full adjustment of the flow to the local irrigated surface. Then the air above the surface still contains properties of the upwind desert. Investigation of this feature requires flux measurements at different heights and at different distances from transition of the dry to the wet fields. During RAPID we did not have such an experimental set-up, so we cannot prove that local

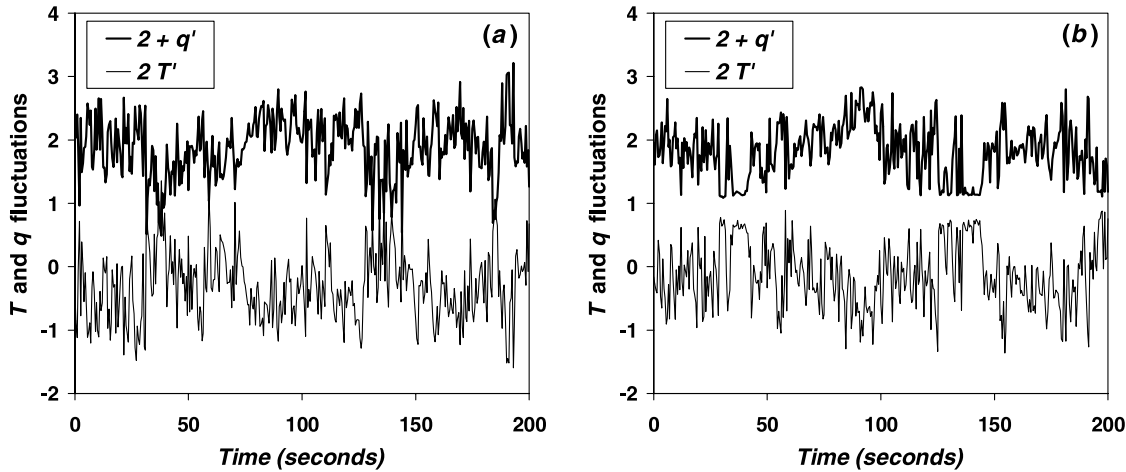


**Fig. 12.** Raw 20 Hz eddy-correlation data taken at 3 m (Fig. 12a) and 10 m (Fig. 12b), sub-sampled at 2 Hz, of temperature,  $T'$ , and humidity,  $q'$ , fluctuations versus time. A record of 200 s is selected between 16:00 and 17:00 on DOY 254. To avoid overlap a constant factor of 2 is added to  $q'$  and  $T'$  is multiplied by 2

advection effects were not present. We collected, however, raw eddy-correlation data at 3 m and at 10 m. In Fig. 12a and b we plotted for a period of 20 seconds the raw temperature and humidity data at 3 and 10 m. Figure 12b shows that the specific humidity at 10 m levels off at some minimum value, whereas at 3 m this effect is not present (see Fig. 12a). For temperature the same can be seen, but now there is a maximum level-off value for the 10 m measurements (Fig. 12b), which is not present in the 3 m measurements. This indicates that the turbulence in the first 3 m was adapted to the irrigated conditions, whereas at 10 m still some upwind ‘desert’ influences were present. Whether this is due to local advection at 10 m is not clear. Inevitably, the dry desert air will be present at greater heights also when the surface layer is fully adapted to the irrigated fields. Due to the nature of atmospheric turbulence individual eddies are expected to penetrated incidentally into the ‘adapted’ surface layer. This will lead to the ‘levelled-off’  $q$ -signal shown in the raw data for 10 m. In a forthcoming paper we will analyse further our RAPID data set in order to investigate the penetration of ‘dry-warm’ events into the adapted surface layer.

## 6. Conclusions

Evapotranspiration,  $\lambda ET$ , of extensive irrigated fields in a desert environment can exceed net radiation under high wind conditions. We base this conclusion on eddy-correlation data taken during the RAPID experiment, which we corrected ac-

cording to the procedure described in Section 2. At night we observed that  $\lambda ET$  can be as large as  $150 \text{ W m}^{-2}$  when the 3 m wind speed exceeds  $6 \text{ m s}^{-1}$ . If such conditions prevail during a whole night,  $ET$  can be as large as 2 mm per night.

We applied a simple model that represents the advection conditions quite well. It is based on a set of governing equations similar to that from which the Penman-Monteith formula has been derived. The model accounts for stability effects in the aerodynamic resistance as well as for the influence of the (calculated) surface temperature on the outgoing long-wave radiation. We tuned the model parameters  $z_{0m}$ ,  $z_{0h}$ ,  $\varepsilon_s$  and  $r_s$  in order to get a fair resemblance between modelled and observed  $H$  and  $\lambda ET$ . This tuned model is able to describe the observed relation between  $H$  and wind speed  $u$  during night-time, which plays a key-role in the advection issue. One might consider applying our adapted Penman-Monteith approach to predict maximum rates of  $\lambda ET$  instead of the Penman-Monteith version now often used for that purpose, which is based on FAO Irrigation and Drainage Paper No. 56 (Allen et al., 1998). However, our model requires hourly standard meteorological data, whereas FAO Penman-Monteith equations require daily averaged data.

We hypothesized that the found high  $\lambda ET$  rates during windy conditions at night-time are due to evaporation of irrigation water. We cannot substantiate this idea with our data, as the observation methods used determine total  $\lambda ET$  and do not distinguish between evaporation of irrigation water and transpiration. At any rate, our results suggest

to recommend farmers not to irrigate if high winds speeds are forecasted, but it is realised that in some windy regions this is impossible.

We found that the correlation coefficient  $R_{uT}$  is a proper indicator for advection conditions. Together with the good correlation found between  $H$  and  $u$ , this feature might be suitable to determine  $\lambda ET$  under night-time advection circumstances. It is suggested to use a 2D sonic anemometer for this purpose, with which  $R_{uT}$  can be determined. More applied research is needed on this issue.

The above results apply to large irrigated fields, where the advected air mass is adapted fully to the surface, and the properties of the upwind desert do not play a role (regional advection). Our data set did not allow studying the flow above small, irrigated fields, where the fetch is small, and the air above the field still contains upwind desert properties (local advection). From the raw data shown in Fig. 12 it can be seen that for that example, the data taken at 3 m height were in a fully adapted layer, whereas at 10 m traces of the upwind desert are present in the data. Local advection might explain the fact that the Kimberly lysimeter data presented in Fig. 1 show daily- $\lambda ET > R_n$  even on calm days.

In this paper we presented some thoughts on the advection issue, which we substantiated with experimental evidence. We used selected cases, however, and a model that was tuned to the measurements. We stress that our results are a first initiative to deal with this issue rather than a final proof and we intend to carry out a more profound study on the RAPID data.

### Acknowledgements

We thank Drs. Larry Hipps, Robert Hill, Christopher Neale, (Utah State University), Dr. James Wright (USDA-ARS, Kimberly) and Dr. Bert Tanner (Campbell Scientific, Inc.) for their valuable contribution to the RAPID field experiment. We highly appreciate the comments Larry Hipps made on the draft of this paper. Dr. James Wright provided the Kimberly lysimeter data presented in Fig. 1. The valuable remarks made by the reviewers are acknowledged also.

### References

Allen RG, Pereira LS, Raes D, Smith M (1998) Crop evapotranspiration (guidelines for computing crop water requirements). FAO Irrigation and Drainage Paper No. 56, 290 pp  
 Allen RG, Pruitt WO, Businger JA, Fritschen LJ, Jensen ME, Quinn FH (1996) Evaporation and transpiration. Chapter 4

in ASCE Hydrology Handbook. New York, NY, pp 125–252  
 Beljaars ACM, Holtslag AAM (1991) On flux parameterization over land surfaces for atmospheric models. *J Appl Meteor* 30: 327–341  
 Bink NJ (1996) The structure of the atmospheric surface layer subject to local advection. Wageningen: PhD Thesis, Wageningen Agricultural University, 206 pp  
 Culf AD, Foken T, Gash JHC (2004) The energy balance closure problem. In: Kabat et al. (eds) *Vegetation, water, humans and the climate. A new perspective on an interactive system*. Berlin, Heidelberg: Springer, pp 159–166  
 De Bruin HAR, Van Den Hurk BJM, Kroon LJM (1999) On the temperature-humidity correlation and similarity. *Bound-Layer Meteorol* 93: 453–468  
 Dyer AJ (1974) A review of flux-profile relationships. *Bound-Layer Meteorol* 7: 453–468  
 Hartogensis OK, DeBruin HAR, Van de Wiel BJH (2002) Displaced-beam small aperture scintillometer test Part II: CASES-99 stable boundary layer experiment. *Bound-Layer Meteorol* 105: 148–176  
 Hoedjes JCB, Zuurbier RM, Watts CJ (2002) Large aperture scintillometer used over a homogeneous irrigated area, partly affected by regional advection. *Bound-Layer Meteorol* 105: 99–117  
 Holtslag AAM, De Bruin HAR (1988) Applied modeling of the night-time surface energy balance over land. *J Appl Meteor* 27: 689–704  
 Kramer JWJL (2000) Surface fluxes in a large irrigated area affected by regional advection. Wageningen: MSc thesis Wageningen University, Meteorology and Air Quality Group, 65 pp  
 Kroon LJM, De Bruin HAR (1995) The Crau field experiment: turbulent exchange in the surface layer under conditions of strong local advection. *J Hydrol* 166: 327–351  
 McNaughton KG, Laubach J (2000) Power spectra and co-spectra for wind and scalars in a disturbed surface layer at the base of an advection inversion. *Bound-Layer Meteorol* 96: 143–185  
 Stewart JB, Kustas WP, Humes KS, Nichols WD, Moran MS, De Bruin HAR (1994) Sensible heat flux-radiative surface temperature relationship for 8 semi-arid areas. *J Appl Meteorol* 33: 1110–1117  
 Van de Wiel BJH, Ronda RJ, Moene AF, DeBruin HAR, Holtslag AAM (2001) Intermittent turbulence and oscillations in the stable boundary layer over land Part I: A bulk model. *J Atmos Sci* 59: 942–958  
 Walter IA, Allen RG, Elliott R, Itenfisu D, Brown P, Jensen ME, Mecham B, Howell TA, Snyder R, Eching S, Spofford T, Hattendorf M, Martin D, Cuenca RH, Wright JL (2002) *The ASCE Standardized Reference Evapotranspiration Equation*. Washington DC: American Society of Civil Engineers, 171 pp

Authors' addresses: H. A. R. De Bruin (e-mail: henk.debruin@wur.nl), O. K. Hartogensis, J. W. J. L. Kramer, Wageningen University, Meteorology and Air Quality Group, Duivendal 2, 6701 AP, Wageningen, The Netherlands; R. G. Allen, University of Idaho at Kimberly Research and Extension Center, Kimberly, Idaho, USA.